

Electronic supplementary information

Direct activation of *Samanea saman* leaves to nitrogen self-doped activation carbons for high energy density supercapacitors

Vichuda Sattayarut,^a Thanthamrong Wanchaem,^a Pundita Ukkakimapan,^a Visittapong Yordsri,^b Paweena Dulyaseree,^c Mayuree Phonyiem,^a Michiko Obata,^d Masatsugu Fujishige,^d Kenji Takeuchi,^{*d} Winadda Wongwiriyan,^{*a} and Morinobu Endo^d

^{a.} College of Nanotechnology, King Mongkut's Institute of Technology Ladkrabang, Chalongkrung Rd., Ladkrabang, Bangkok 10520, Thailand. *Email: winadda.wo@kmitl.ac.th.

^{b.} Thailand National Metal and Materials Technology Center, Phahonyothin Rd., Khlong Luang, Pathumthani 12120, Thailand.

^{c.} Department of Physics, Faculty of Science Technology and Agriculture, Yala Rajabhat University, 133 Thesaban 3, Sateng, Muang, Yala, 95000

^{d.} Institute of Carbon Science and Technology, Shinshu University, 4-17-1 Wakasato, Nagano, 380-8553, Japan. *Email: takeuchi@endomoribu.shinshu-u.ac.jp.

1. Elemental composition of the *Samanea saman* leaves (SSL) before and after H₂SO₄ treatment

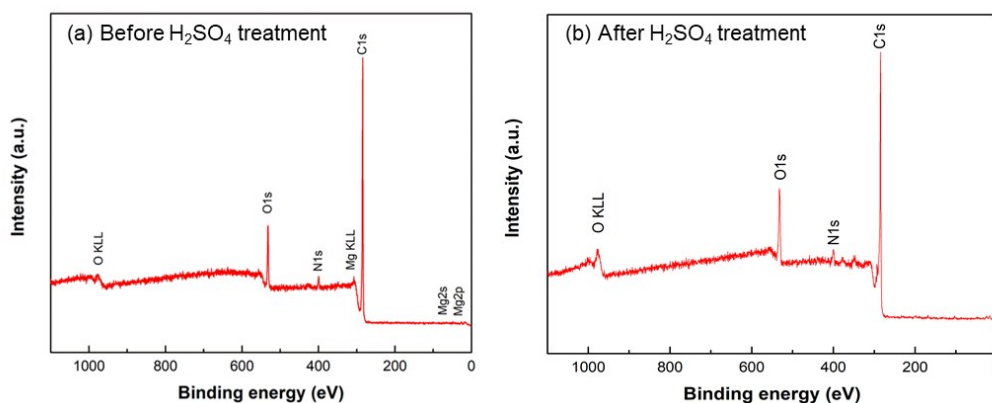


Fig. S1 XPS survey scan of the *Samanea saman* leaves (SSL) (a) before (raw material) and (b) after H₂SO₄ treatment

Table S1. Summary of XPS peak analysis of the SSL before and after H₂SO₄ treatment

SAMPLE	CONTENT (AT%)					C/N RATIO (%)	O/N RATIO
	C	N	O	Mg	S		
Before	83.3	3.2	12.4	0.9	0.2	3.8	3.9
After	81.8	4.7	13.1	<0.08	<0.2	5.2	1.5

It was found that the main elemental composition of SSLs were carbon, nitrogen, oxygen, magnesium and sulfur. Interestingly, the atomic ratio of nitrogen to magnesium is approximately 3.6, corresponding to the molecular structure of chlorophyll that is four pyrrole rings containing nitrogen arranged in a ring around a magnesium ion, and a long hydrocarbon tail.

The purpose of the pre-treat of biomass leaves by using H₂SO₄ under 100°C is to remove inorganic compositions such as magnesium. Magnesium sulfate is dissolved in water and removed from biomass as confirmed in Fig. S1b and Table S1.

2. XRD pattern of activated carbons

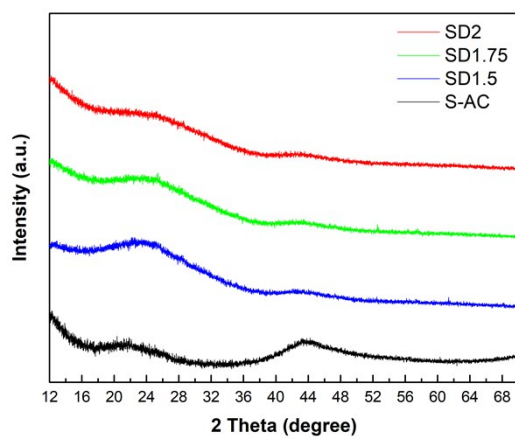


Fig. S2 XRD patterns of SD-ACs and S-AC.

3. C1s XPS spectra of activated carbon

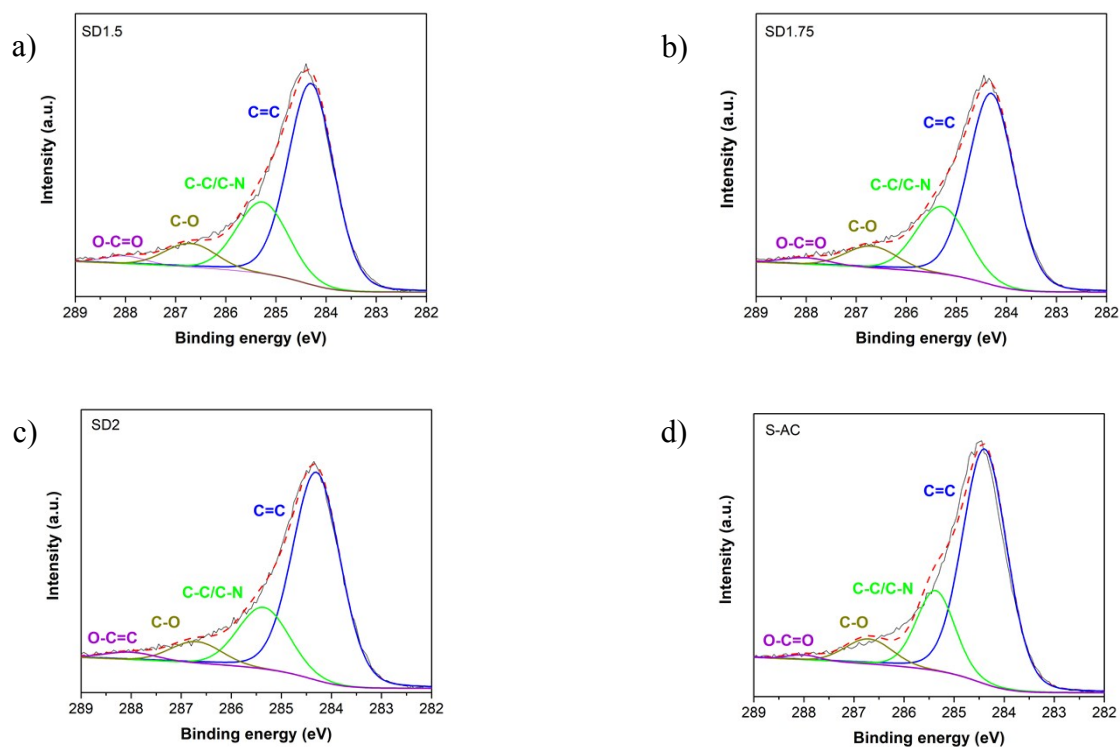


Figure S3. C1s XPS spectra of SD1.5, SD1.75, SD2 and S-AC samples

Table S2. XPS peak analysis of the all samples

Samples	Element content (at%)			Relative C1s peak area (at%)			
	C	O	N	C = C	C - C / C - N	C - O	O - C = O
SD-AC	90.6	7.7	1.7	64.07	18.76	6.80	0.89
SD1.5	86.7	9.7	3.6	56.50	21.42	6.94	1.83
SD1.75	87.6	8.2	4.2	57.82	21.33	6.68	1.78
SD2	88.4	7.0	4.6	61.40	18.52	6.30	2.17

4. O1s XPS spectra of activated carbon

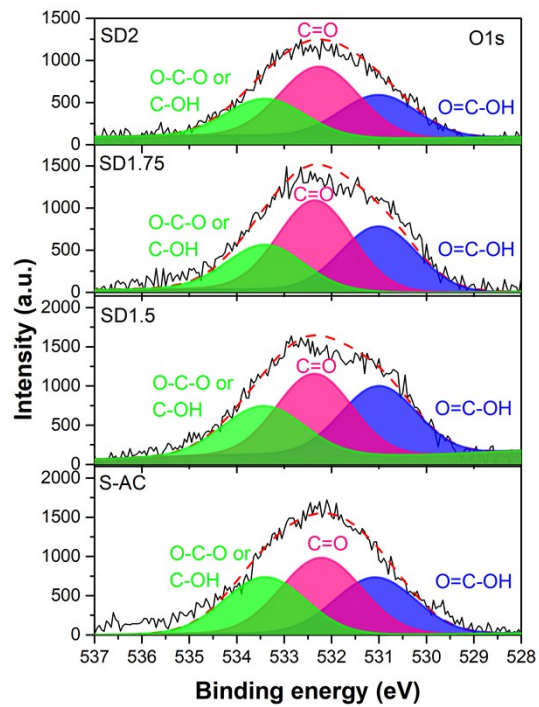


Fig. S4 O1s XPS spectra of SD1.5, SD1.75, SD2 and S-AC samples

5. Electrochemical properties of activated carbons in an aqueous electrolyte (1 M Na₂SO₄)

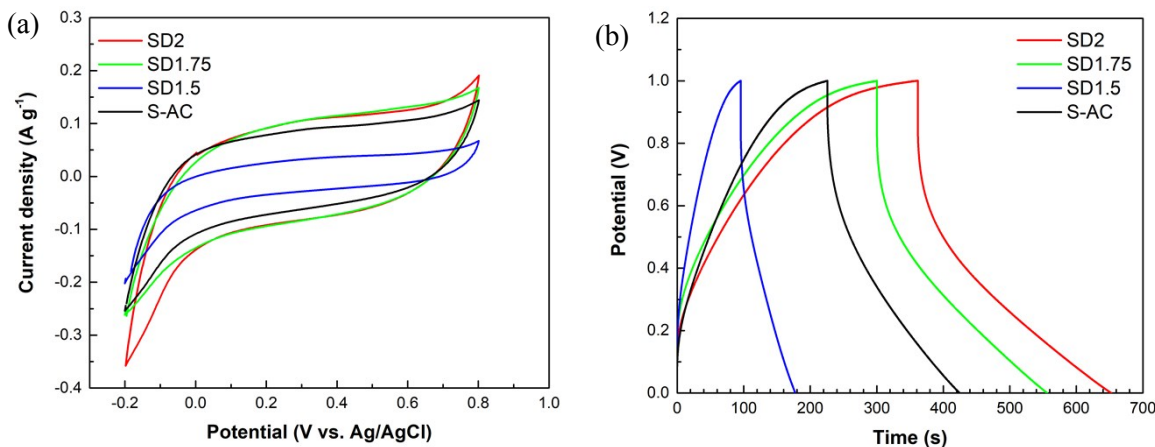


Fig. S5 Electrochemical properties of SD1.5, SD1.75, SD2 and S-AC in 1 M Na₂SO₄ aqueous electrolyte: (a) CV curves, (b) CD curves

The electrochemical properties were also measured in aqueous electrolyte using three-electrode system. The activated carbon was used as a working electrode on Ni foam as a current collector. The Pt and Ag/AgCl were used as counter and reference electrodes, respectively, and 1 M Na₂SO₄ aqueous solution was used as an electrolyte. Fig. S5 shows CV and CD curves of each electrode.

Fig. S5a exhibited CV curves of all samples at a scan rates of 1 mVs⁻¹ in the potential window range of -0.2 – 0.8 V. Fig. S5b shows galvanostatic CD curves in the potential range of 0.0 – 1.0 V at the current density of 0.3 Ag⁻¹. All CD curves are quasi-triangular shape and nearly linear response, indicating good electrochemical reversibility and supercapacitive behavior. The value of the gravimetric capacitances of each electrode calculated from CD curves were in the following order: SD2 (322.6 Fg⁻¹) > SD1.75 (280.4 Fg⁻¹) > S-AC (205.1 Fg⁻¹) > SD1.5 (82.8 Fg⁻¹).

The SD2 shows the highest gravimetric capacitance owing to the highest surface area, the highest volumes of micro- and meso-pores, and the highest nitrogen content. Interestingly, the SD1.75 shows the higher gravimetric capacitance even though its lower surface capacitance than the S-AC. On the other hand, the SD1.5 shows the lowest gravimetric capacitance even though its higher nitrogen content than the S-AC. These results show that the high performance of the electrode is attributed to the synergistic effects of the highest surface area and highest nitrogen content.

5. Comparison of electrochemical performance

Precursors	Carbonization	Activation agent	Activation temperature/time (°C/h)	SSA ^a (m ² g ⁻¹)	C _S ^b (F g ⁻¹)	I _D ^c (A g ⁻¹)	Electrolyte *	Max E ^d (Wh kg ⁻¹)	Max P ^e (W kg ⁻¹)	Voltage (V)	Ref.
Silkworm pupae	HTC	ZnCl ₂	800/1	1188	91	0.2	1 M TEABF ₄ /PC	17.5	1698	2.5	19
Tobacco rods	HTC	KOH	900/1	2097	144	0.5	CH ₃ (C ₂ H ₅) ₃ NBF ₄ /AN	31.3	625	2.5	20
Wheat bran	HTC	KOH	800/1	2189	129	0.25	1 M TEABF ₄ /AN	32.7	1351	2.7	21
Green leaves	Pyrolysis/600	NaOH	720/1	2664	188	0.02	1 M TEABF ₄ /PC	39	1700	2.5	22
Paper pulp	HTC	KOH	800/1	2980	166	0.1	1 M TEABF ₄ /AN	30	57	3.0	23
Silkworm cocoon	Pyrolysis/500	KOH	900/2	3386	156	5	1 M TEABF ₄ /AN	34.4	3125	2.4	24
Seaweeds	Pyrolysis/900	-	-	1307	94	1	1 M TEABF ₄ /AN	17.3	1150	2.3	25
Rice husk	-	Microwave assisted ZnCl ₂	600 W	1552	94	0.05	1 M TEABF ₄ /PC	19.3	1007	2.7	26
Coconut shell	-	ZnCl ₂ +FeCl ₃	900/1	1874	196	1	1 M TEABF ₄ /PC	54.7	10000	3.0	27
Onion husks	-	K ₂ CO ₃	800/1	2571	188	0.5	1 M TEABF ₄ /AN	47.6	675	2.7	28
<i>S. saman</i> leaves	-	NaOH	720/1	2930	179	0.02	1 M TEABF ₄ /PC	79	830	3.5	This work

Table S3. Comparison of electrochemical performance in organic electrolyte of this work and other recently works

^a SSA: Specific surface area. ^b C_S: Specific capacitance. ^c I_D: Current density. ^d E: Energy density. ^e P: Power density.

*Electrolyte: TEABF₄/PC: Tetraethylammonium tetrafluoroborate in propylene carbonate, TEABF₄/AN: Tetraethylammonium tetrafluoroborate in acetonitrile, CH₃(C₂H₅)₃NBF₄/AN: Triethyl-methyl-ammonium tetrafluoroborate in acetonitrile

